RadioGraphics

Understanding Diffusion MR Imaging Techniques: From Scalar Diffusion-weighted Imaging to Diffusion Tensor Imaging and Beyond[1]

Patric Hagmann, MD, PhD • Lisa Jonasson, PhD • Philippe Maeder, MD
Jean-Philippe Thiran, PhD • Van J. Wedeen, MD • Reto Meuli, MD, PhD

TEACHING POINTS
See last page

The complex structural organization of the white matter of the brain can be depicted in vivo in great detail with advanced diffusion magnetic resonance (MR) imaging schemes. Diffusion MR imaging techniques are increasingly varied, from the simplest and most commonly used technique—the mapping of apparent diffusion coefficient values—to the more complex, such as diffusion tensor imaging, q-ball imaging, diffusion spectrum imaging, and tractography. The type of structural information obtained differs according to the technique used. To fully understand how diffusion MR imaging works, it is helpful to be familiar with the physical principles of water diffusion in the brain and the conceptual basis of each imaging technique. Knowledge of the technique-specific requirements with regard to hardware and acquisition time, as well as the advantages, limitations, and potential interpretation pitfalls of each technique, is especially useful.

Abbreviations: ADC = apparent diffusion coefficient, SE = spin echo, 6D = six-dimensional, 3D = three-dimensional

RadioGraphics 2006; 26:S205–S223 • **Published online** 10.1148/rg.26si065510 • **Content Codes:** MR NR PH

[1]From the Department of Radiology, Lausanne University Hospital (CHUV), Rue du Bugnon, 46, CH-1011 Lausanne, Switzerland (P.H., P.M., R.M.); Signal Processing Institute, École Polytechnique Fédérale de Lausanne, Lausanne, Switzerland (P.H., L.J., J.P.T.); and MGH Martinos Center for Biomedical Imaging, Harvard Medical School, Charlestown, Mass (V.J.W.). Recipient of an Excellence in Design award for an education exhibit at the 2005 RSNA Annual Meeting. Received February 28, 2006; revision requested April 21 and received May 25; accepted June 9. All authors have no financial relationships to disclose. Supported by Swiss National Science Foundation 2153-066943.01 and 3235B0-102863, by NIH 1R01-MH64044, and by Yves Paternot. **Address correspondence to** P.H. (e-mail: *patric.hagmann@epfl.ch*).

Introduction

Diffusion-weighted magnetic resonance (MR) imaging, boosted by established successes in clinical neurodiagnostics and powerful new applications for studying the anatomy of the brain in vivo, has been an important area of research in the past decade. Current clinical applications are based on many different types of contrast, such as contrast in relaxation times for T1- or T2-weighted MR imaging, in time of flight for MR angiography, in blood oxygen level dependency for functional MR imaging, and in diffusion for apparent diffusion coefficient (ADC) imaging. Even more advanced techniques than these are in use today for the study of neural fiber tract anatomy and brain connectivity.

Over the years, increasingly complex data acquisition schemes have been developed, while the theoretical foundations of diffusion MR imaging have come to be better understood. For the radiologist who wants to use these techniques in clinical practice and research, it is important to understand a few key principles of diffusion imaging so as to select the appropriate technique for answering a specific question. The article therefore begins with an explanation of the physics of water diffusion and the ways in which the great complexity of diffusion in the brain, the main organ targeted for investigation with diffusion MR imaging, can be described. Next, the basic principles that underlie diffusion contrast encoding with MR imaging are described to enable the reader to understand the relation between the MR imaging signal and diffusion as well as the limitations of simple diffusion imaging techniques. This discussion provides a context for the description of diffusion spectrum imaging, the most complex diffusion MR imaging technique, which provides the largest body of information and the greatest detail. With the general principles of diffusion MR imaging in mind, the range of current diffusion MR imaging techniques, from the simplest to the most sophisticated, is then reviewed with an emphasis on the underlying assumptions and hypotheses, advantages, and potential pitfalls of each. The technical requirements (hardware capabilities, acquisition time) for each type of diffusion imaging examination, and the types of data provided by each type, are compared.

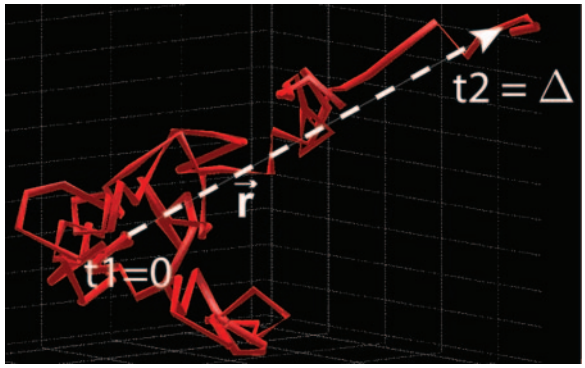

Figure 1. Diagram shows the diffusion-driven random trajectory (red line) of a single water molecule during diffusion. The dotted white line (vector **r**) represents the molecular displacement during the diffusion time interval, between $t_1 = 0$ and $t_2 = \Delta$.

The Physics and Representation of Diffusion

Molecular diffusion, or brownian motion, was first formally described by Einstein in 1905 (1). The term *molecular diffusion* refers to the notion that any type of molecule in a fluid (eg, water) is randomly displaced as the molecule is agitated by thermal energy (Fig 1). In a glass of water, the motion of the water molecules is completely random and is limited only by the boundaries of the container. This erratic motion is best described in statistical terms by a displacement distribution. The displacement distribution describes the proportion of molecules that undergo displacement in a specific direction and to a specific distance.

Teaching Point

To illustrate this idea, we can perform an imaginary experiment. Let us imagine that we launch, at time $t = 0$, a given number N of labeled water molecules in water, and we measure their individual displacement after a given time interval Δ (hereafter, diffusion time interval). For each displacement distance **r**, we count the number n of labeled water molecules that are displaced that distance. We use the resultant data to plot a histogram of the relative number of labeled molecules (n/N) versus displacement distance (**r**) in a single direction. Most of the molecules travel short distances, and only a few travel farther (Fig 2). Typically, the displacement distribution for free water molecules is a Gaussian (bell-shaped) function. At 37°C, with a diffusion time interval of $\Delta = 50$ msec, the characteristic distance (standard deviation of the Gaussian distribution) typically is 17 μm, which means that about 32% of the molecules have moved at least this far, whereas only 5% of them have traveled farther than 34 μm (2).

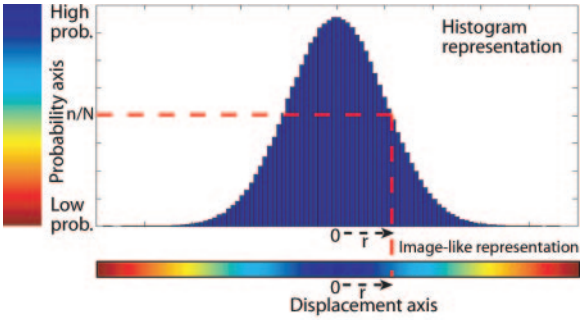

a.

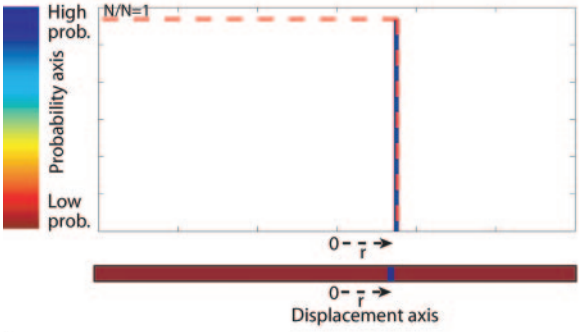

b.

Figure 2. **(a)** Histogram shows a typical displacement distribution due to diffusion in a one-dimensional model. For each displacement distance **r** (x-axis) there is a corresponding probability n/N (y-axis), which is the proportion of molecules within a voxel that were displaced that distance within a time interval Δ (the duration of the diffusion experiment). The top of the histogram is centered on zero, indicating that most molecules had the same position at $t = 0$ and $t = \Delta$. The proportion of molecules that traveled the given distance **r** is indicated by the dotted red line. The horizontal color bar, in which blue signifies a high probability and red a low probability of displacement, shows the same Gaussian distribution. **(b)** Histogram shows a typical displacement distribution due to flux (ie, nonzero average displacement). All the molecules have moved the given distance **r**, as shown by $N/N = 1$.

A histogram like that in Figure 2 is adequate for the display of one-dimensional data, but it is not practical for visualizing displacement in multiple dimensions. A useful approach is instead to color-code the probability. With such a representation, the one-dimensional problem can be visualized as a colored displacement axis (x-axis) in which blue codes for high and red for low probability (Fig 2). According to this rule, we can represent actual three-dimensional (3D) diffusion as a 3D image in which the probability of displacement in three intersecting planes is coded in color (Fig 3a). The central voxel of the image is the origin, and its value codes for the probability, or the proportion of molecules (n/N) that do not

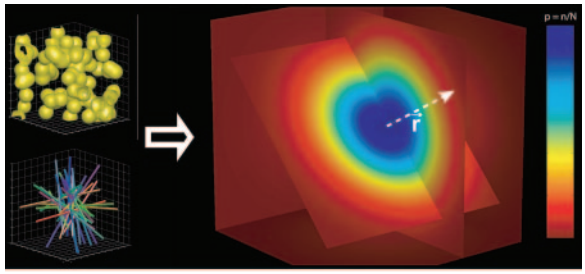

a.

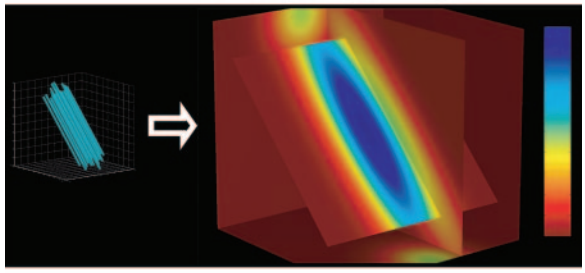

b.

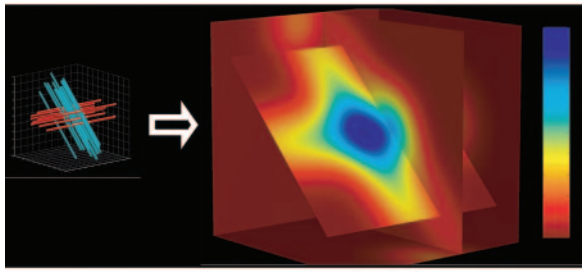

c.

Figure 3. Diffusion within a single voxel. **(a)** Diagram shows the 3D diffusion probability density function in a voxel that contains spherical cells (top left) or randomly oriented tubular structures that intersect, such as axons (bottom left). This 3D displacement distribution, which is roughly bell shaped, results in a symmetric image (center), as there is no preferential direction of diffusion. The distribution is similar to that in unrestricted diffusion but narrower because there are barriers that hinder molecular displacement. The center of the image (origin of the **r** vector) codes for the proportion of molecules that were not displaced during the diffusion time interval. The color bar (right) shows the spectrum used in color coding to represent probability, from the lowest value, which is indicated by red, to the highest, which is indicated by blue. **(b)** Diagram shows the diffusion probability density function within a voxel in which all the axons are aligned in the same direction. The displacement distribution is cigar shaped and aligned with the axons. **(c)** Diagram shows the diffusion probability density function within a voxel that contains two populations of fibers intersecting at an angle of 90°. The molecular displacement distribution produces a cross shape.

undergo displacement between $t = 0$ and $t = \Delta$. This 3D diagram represents the displacement distribution. A simple practical analogy is a drop of dye falling in a glass of water. On a photograph taken at $t = \Delta$, the dye will have been diluted (diffused), and the relative color density will indicate the proportion of dye molecules displaced a given distance.

Diffusion in a homogeneous medium is well described as having a Gaussian distribution. Depending on the type of molecule, the temperature of the medium, and the time allowed for diffusion, the distribution will be wider or narrower. The spread of the Gaussian distribution is controlled by a single parameter: variance (σ^2). Variance, in turn, depends on two variables, so that $\sigma^2 = 2 \cdot D \cdot \Delta$, where D, the diffusion coefficient, characterizes the viscosity of the medium or the ease with which molecules are displaced. The diffusion coefficient for water at 37°C is approximately $D = 3 \cdot 10^{-9}$ m^2/sec. The longer the diffusion time interval, the larger the variance, because there is more time in which molecules may be displaced.

Molecular Displacement, Diffusion, and Flux

To describe the global behavior of a population of water molecules contained in an imaging voxel, we use the term *displacement distribution*. Equivalent terms to the latter are *displacement probability density function* and *image of molecular displacement*. In the present article, these terms are used interchangeably. When molecules are agitated by thermal energy alone (ie, when molecular displacement takes place through the process of diffusion), the displacement distribution is centered. This means that the average or net displacement of the molecular population is zero. Factors other than heat also may contribute to molecular displacement. For example, a pressure gradient in a pipe may affect molecular displacement. In an ideal setting with no turbulence and no friction, all molecules undergo the same nonzero displacement **r**. Such a setting produces a very different displacement distribution, in which the histogram is zero everywhere except in the position **r**, which has the value $N/N = 1$ (Fig 2b) because all the molecules have been displaced the same distance. This type of displacement is called flux. In flux, molecules are displaced over a nonzero average distance. Although diffusion and flux may occur together, for the sake of simplicity we have chosen in the present article to focus on diffusion only.

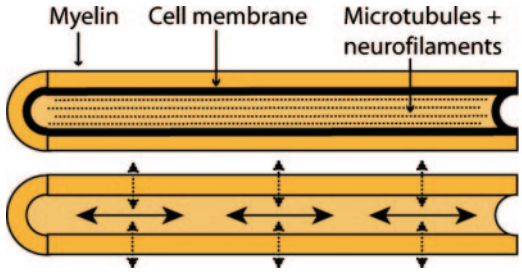

Figure 4. Diagram shows the cellular elements that contribute to diffusion anisotropy.

Therefore, the word *displacement* is often replaced with the more specific term *diffusion.*

Diffusion in a Complex Medium

As mentioned earlier, a water molecule in a glass of water moves randomly and, given sufficient time, may circumnavigate the internal contents of the glass but cannot go beyond it. The same is true for water molecules within impermeable spheres that may be introduced into the glass of water (Fig 3a). The water molecules inside each sphere diffuse within the restricted space of that sphere, and the water molecules outside the spheres move randomly around them. Accordingly, the displacement distribution associated with a volume (ie, voxel) that contains the impermeable spheres and their surround will be rather different from that associated with the same volume before the spheres were introduced. The difference reflects the presence of water restriction. Because molecules inside the sphere cannot move beyond its boundaries, and because molecules outside cannot penetrate the sphere, the expected displacement distance is reduced. It is difficult to predict the shape of the resultant displacement distribution, but it will be more or less bell shaped and markedly narrower than that for unrestricted diffusion, if the diffusion time interval is sufficiently long (Fig 3a). As in free diffusion, the displacement is isotropic, with no preferential direction. To approximate the biological reality, one could introduce into the glass of water a population of semipermeable spheres with a membrane that water molecules can cross with some resistance. Such intermediate conditions will produce a displacement distribution that is not as narrow as that for a volume containing impermeable spheres but narrower than that for a volume with free diffusion.

Biological tissues are highly heterogeneous media that consist of various compartments and barriers of different diffusivities. In terms of its cytohistologic architecture, a tissue can be regarded as a porous structure made up of a set of more or less connected compartments in a networklike

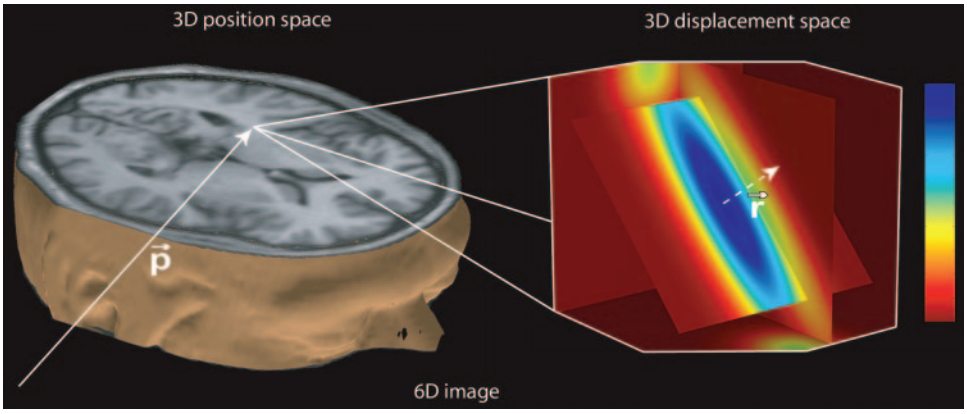

Figure 5. Left part of diagram shows that standard imaging methods provide one value (gray level) for every 3D position **p**. That value or gray level may code for the linear x-ray attenuation coefficient at CT or for the relative signal intensity at MR imaging. Right part of diagram shows that in diffusion imaging every 3D position **p** (voxel) is associated not with a gray level but with a 3D image that encodes the molecular displacement distribution in that voxel. The value measured at the coordinates **p**,**r**—f(**p**,**r**)—indicates the proportion of molecules in the voxel that have moved the given distance **r**.

arrangement. The movement of water molecules during diffusion-driven random displacement is impeded by compartmental boundaries and other molecular obstacles in such a way that the actual diffusion distance is reduced, compared with that expected in unrestricted diffusion. A defining characteristic of neuronal tissue is its fibrillar structure. Neuronal tissue consists of tightly packed and coherently aligned axons that are surrounded by glial cells and that often are organized in bundles. As a result, the micrometric movements of water molecules are hindered to a greater extent in a direction perpendicular to the axonal orientation than parallel to it (Fig 3b). Consequently, molecular displacement parallel to the fiber typically is greater than that perpendicular to it. When diffusive properties change with the direction of diffusion, the prevailing condition is anisotropy, and the associated displacement distribution is no longer isotropic and Gaussian, like that in unrestricted diffusion, but cigar shaped. Of course, the distribution may be even more complicated if the underlying tissue contains fibers with various orientations (Fig 3c) (3).

Teaching Point

Experimental evidence suggests that the tissue component predominantly responsible for the anisotropy of molecular diffusion observed in white matter is not myelin, as one might expect, but rather the cell membrane (4) (Fig 4). The degree of myelination of the individual axons and the density of cellular packing seem merely to modulate anisotropy. Furthermore, axonal transport, microtubules, and neurofilaments appear to play only a minor role in anisotropy measured at MR imaging (4).

Diffusion Represented by a Six-dimensional Image

The image data acquired with computed tomography (CT) or MR imaging are usually 3D data. Every position in 3D space is associated with a gray level that encodes the linear attenuation coefficient at CT or the relative signal intensity at MR imaging. In mathematical terms, the 3D image is a function of the position variable **p** (a 3D vector) and is designated as f(**p**). Furthermore, the brain is a highly compartmentalized and heterogeneous medium, with a different cytoarchitecture in different locations. Accordingly, if the local displacement distribution were measured in various brain locations (voxels), there would be as many different 3D displacement distributions as there are voxels. To describe diffusion properly in such a medium, every voxel position **p** must be assigned a diffusion probability density function (equivalent to the displacement distribution). Since the visual representation of a diffusion probability density function is a 3D image, the natural result of the combination of the two variables **p** and **r** is a six-dimensional (6D) image. The 6D image fully characterizes diffusion in a heterogeneous medium, as it depicts the proportion of molecules f(**p**,**r**) in voxel position **p** that have been displaced a distance **r** (Fig 5). In other words, instead of each individual position being assigned a single gray level as in CT or standard MR imaging, each position **p** is associated with a new 3D image on which molecular displacement is encoded. The resultant 6D image represents the function of three position variables

(3D position vector **p**) and three displacement variables (3D displacement vector **r**). This concept of multidimensionality may not be intuitive to nonspecialists in mathematics but is nonetheless essential for understanding diffusion imaging.

Representing 6D Data in Three Dimensions

In standard 3D imaging, there is little difference between the data that are a function of position **p** and their representation on the display monitor as a section in which the function intensity is encoded in gray levels. However, the distinction between the two is more important when the data are six dimensional, as six dimensions cannot be represented straightforwardly in a single section; specific computer visualization techniques must be used to reduce the overwhelming amount of information in six dimensions to the most important features. Typically, at diffusion imaging, there is less interest in obtaining a detailed diffusion profile than in determining the direction of the most rapid diffusion, because the latter parameter likely corresponds to the orientation of axons or other fibrillar structures. One possible approach would be to replace the diffusion probability density function with an isosurface, which is a surface that passes through all points of equal value, or, in other words, where the value of $f(\mathbf{r})$ is a constant (Fig 6). A more commonly used technique that is less sensitive to noise involves the computation of the orientation distribution function from the displacement distribution (Figs 6, 7). An orientation distribution function may be considered a deformed sphere whose radius in a given direction is proportional to the sum of values of the diffusion probability density function in that direction. For ease of visualization, we color code the surface according to the diffusion direction ($[x,y,z] = [r,b,g]$, where r = red, b = blue, and g = green). An orientation distribution function or isosurface can be plotted for each individual MR imaging voxel in a section (Fig 8).

Teaching Point

A General Description of Diffusion Contrast Encoding

To depict the displacement distribution, diffusion must be linked to the signal intensity measured at

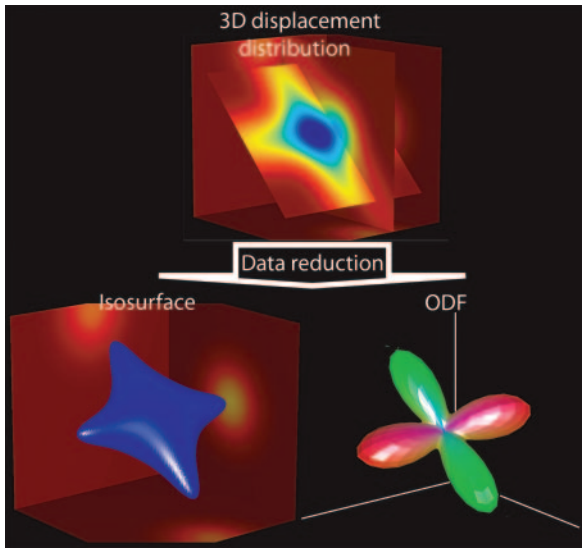

Figure 6. Diagram shows two approaches that may be used to simplify the visual representation of 3D diffusion data: replacement of the displacement distribution with an isosurface, and computation of the orientation distribution function *(ODF)*.

MR imaging. As previously mentioned, water molecules move randomly in the presence of thermal energy. In 1950, Hahn noted that the motion of spins (ie, hydrogen protons of the water molecule) in the presence of a heterogeneous magnetic field led to a decrease in signal intensity (5). In 1956, Torrey established the fundamental equations used to describe the magnetization of spins in an MR spectroscopy experiment (6). Since then, these equations have come to be regarded as the most fundamental equations in diffusion imaging.

The results of the first MR spectroscopy experiment specifically designed to measure diffusion were reported in 1965 by Stejskal and Tanner (7). In their experiment, the investigators used a pulsed gradient spin-echo (SE) sequence, a technique based on the observation that spins moving in the magnetic field gradient direction are exposed to different magnetic field strengths depending on their position along the gradient axis. As is well known in MR imaging, an adequately applied magnetic field influences the phase of the spins, with the degree of influence depending on the strength of the field. Compared with a classic SE sequence, the pulsed gradient SE sequence includes two additional diffusion

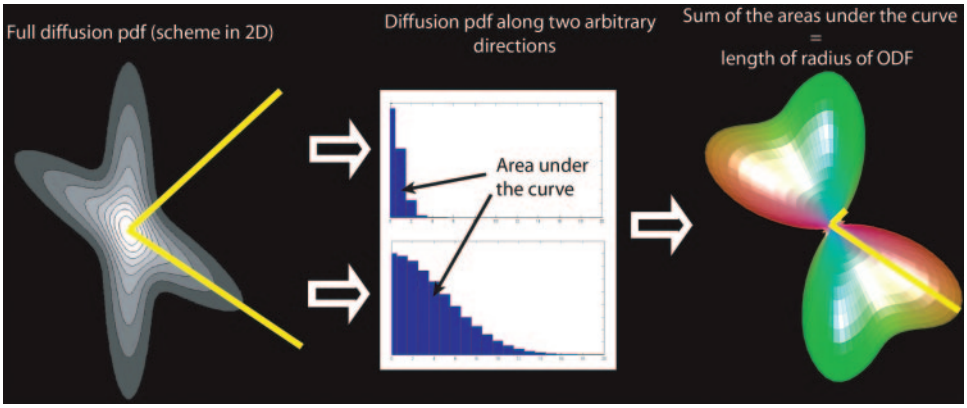

Figure 7. Diagram shows how an orientation distribution function *(ODF)* is computed and represented. Left: Image of a section through a schematized 3D displacement distribution. The value of the orientation distribution function was computed along two axes (yellow lines). Center: Histograms represent the displacement distribution along the two axes. The value of the orientation distribution function along those axes equals the area under the curve for each axis. In this example, the two areas under the curve are respectively small and large, indicating that there is much less diffusion in the one direction than in the other. Right: The sum of the areas under the curve is represented by a deformed sphere in which the lengths of the two radii (yellow lines) are short and long, corresponding to little diffusion and much diffusion, respectively. To compute the orientation distribution function, the area under the curve is computed for every direction.

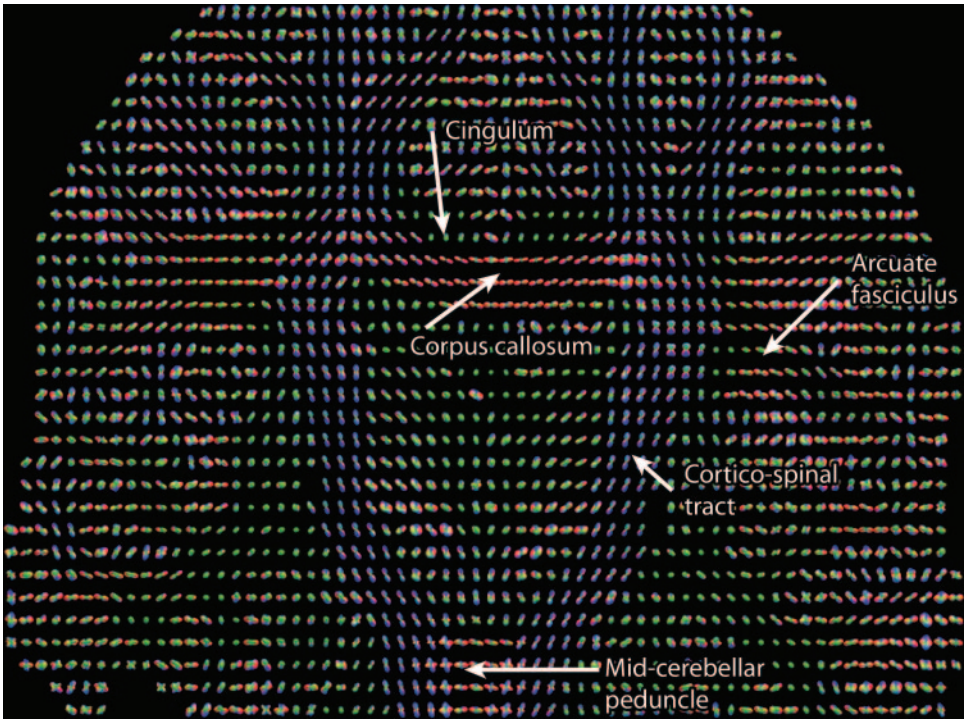

Figure 8. Orientation distribution function map of a coronal brain section. For every brain position **p**, an orientation distribution function is plotted to characterize the local diffusion probability density function. It is easy to identify the corticospinal tract, in which the dominant color is blue, and the corpus callosum, in which red is predominant. More difficult to see are the cingulum and the arcuate fasciculus, depicted predominantly in green, and the middle cerebellar peduncle, in red.

gradient pulses (Fig 9). The first of the two gradient pulses in this sequence introduces a phase shift that is dependent on the strength of the gradient at the position of the spin at $t = 0$. Before the application of the second gradient pulse, which induces a phase shift dependent on the spin position at $t = \Delta$, a 180° RF pulse is applied to reverse the phase shift induced by the first gradient pulse. Since the diffusion-encoding gradient causes the field intensity (ie, phase shift) to vary with position, all spins that remain at the same location along the gradient axis during the two pulses will return to their initial state. However, spins that have moved will be subjected to a different field strength during the second pulse and therefore will not return to their initial state but will experience a total phase shift that results in decreased intensity of the measured MR spectroscopic signal. The longer the displacement distance is, the higher the phase shift and the greater the decrease in signal will be. Hence, the resultant image shows low signal intensity in regions where diffusion along the applied diffusion gradient is high.

A diffusion gradient can be represented as a 3D vector **q** whose orientation is in the direction of diffusion and whose length is proportional to the gradient strength. The gradient strength, or more often the diffusion weighting, is sometimes expressed in terms of the *b* value, which is proportional to the product of the square of the gradient strength *q* and the diffusion time interval ($b \sim q^2 \cdot \Delta$).

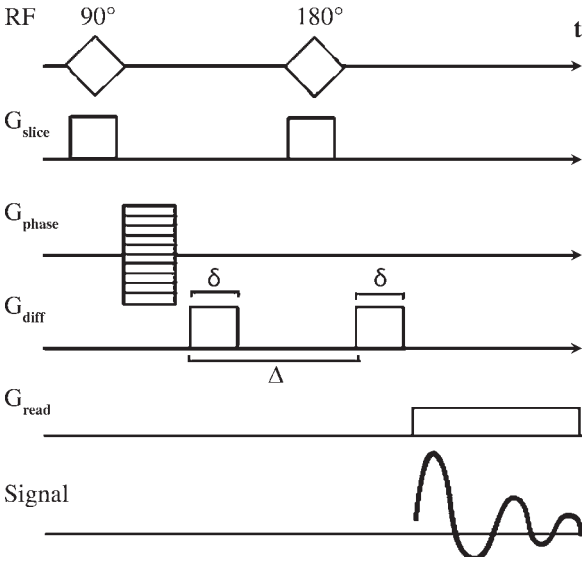

Figure 9. Diagram shows the pulsed gradient SE sequence used for diffusion MR imaging. Two diffusion-encoding gradient *(G_{diff})* pulses are added to the standard SE MR imaging sequence to introduce a phase shift proportional to molecular displacement along the gradient direction. δ = duration of the diffusion-encoding gradient, *Δ* = diffusion time interval, G_{phase} = phase-encoding gradient, G_{read} = readout gradient, G_{slice} = section-selective gradient, *RF* = radiofrequency pulse, *t* = acquisition time. The diffusion-encoding gradient often is symbolized by the vector **q**, which is equal to the product of $\gamma \cdot \delta \cdot \mathbf{G}_{diff}$, where γ is the gyromagnetic ratio; thus, it represents the effective diffusion gradient.

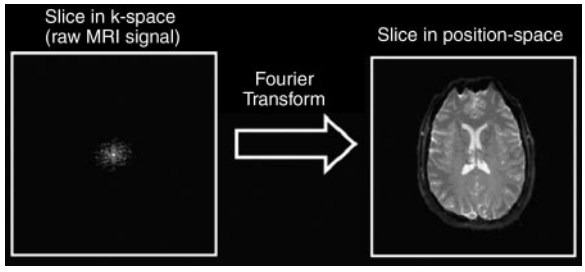

Figure 10. Diagram shows the process with which a standard position-encoded MR image is obtained. First, the MR signal that was generated by the application of phase- and frequency-encoding gradients is sampled to fill k-space (a coordinate system used to organize the signal measurements). Next, the raw data (k-space images) are subjected to a mathematical operation known as a Fourier transform to reconstruct an image in the standard position space.

q-Space Explained in Analogy to k-Space

According to basic MR imaging principles (8,9), the measured signal at conventional MR imaging is phase and frequency encoded. It is the result of the application of gradients in different directions and with different intensities at specific moments of the acquisition sequence. The values of the measured signal are organized in a coordinate system known as k-space. Performing the acquisition enables the filling of k-space. To transform the raw MR imaging data from k-space into a position-encoded visual image, a mathematical operation known as a Fourier transform is applied (Fig 10) (9,10).

The process in diffusion MR imaging is analogous. Let us first define a new 3D space, called q-space, the coordinates of which are defined by a vector **q** (11). The application of a single pulsed gradient SE sequence produces one diffusion-weighted image that corresponds to one position in q-space or, more precisely, that depicts the diffusion-weighted signal intensity in a specific position **q** for every brain position. Repeated applications of the sequence with gradients that vary in strength and in direction (ie, with variations of **q**) allow data sampling throughout q-space. Like the data from conventional MR imaging, in which a Fourier transform is applied to the data in

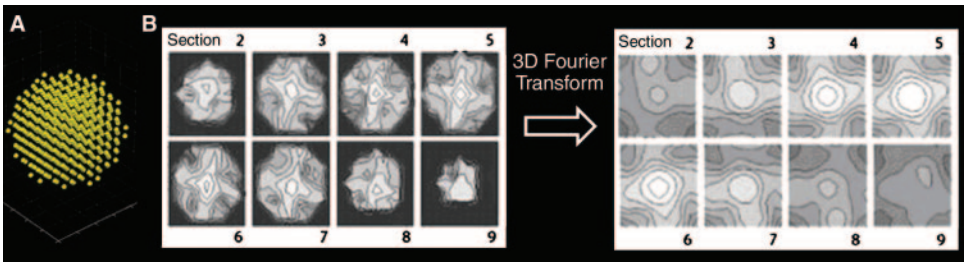

Figure 11. Diagram shows the process with which a 3D diffusion probability density function is obtained for one voxel (one brain position). In *A*, a 3D grid that represents q-space, each yellow dot corresponds to an MR signal sampling point. The signal is sampled at each point by varying the direction and strength of the diffusion gradient (**q** vector) of the pulsed gradient SE sequence. With a single application of the pulsed gradient SE sequence, one point in q-space is sampled for each brain position simultaneously, and the result is one diffusion-weighted image. In *B*, the left panel shows sections through the MR signal sampled in q-space for a specific brain position (one voxel), and the right panel shows the diffusion probability density function in the same voxel after a 3D Fourier transform of the MR signal in q-space is performed. The cross-shaped appearance of the diffusion probability density function is often seen in voxels in the brainstem, where axons of the corticospinal tract cross with axons of the middle cerebellar peduncle.

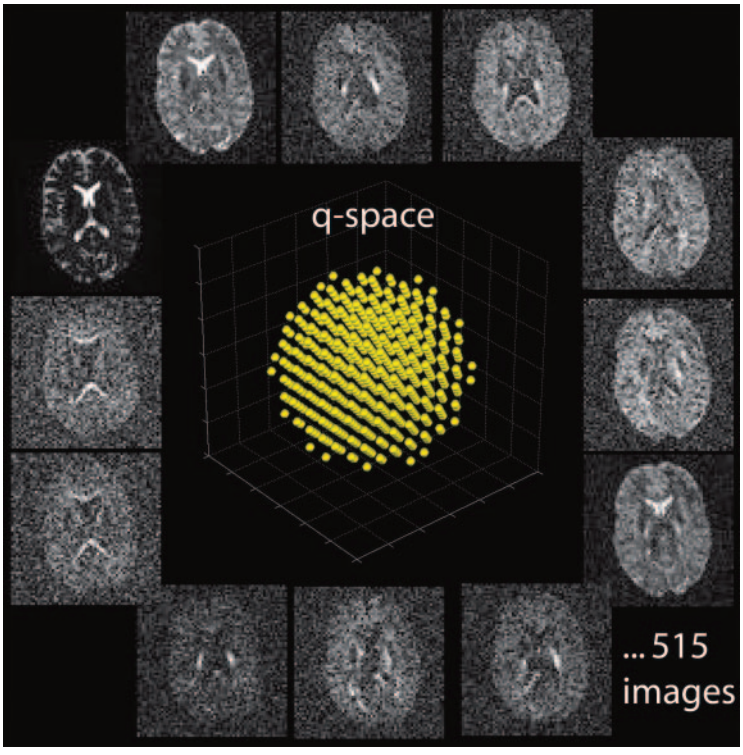

Figure 12. Series of diffusion-weighted MR brain images obtained with variations in the direction and strength of the diffusion gradient in the pulsed gradient SE sequence. Each image shows the signal sampled at one point in q-space (one yellow dot). Every sampling point in q-space corresponds to a specific direction and strength of the diffusion gradient.

k-space, the q-space data are subjected to a Fourier transform in every brain position. The result is a displacement distribution in each brain position (ie, voxel) (Fig 11). In other words, a single application of the pulsed gradient SE sequence produces one brain image with a given diffusion weighting. Multiple repetitions of the sequence, each with a different diffusion weighting, are necessary to sample the entirety of q-space; the result is hundreds of brain images, each of which reflects the particular diffusion weighting used. One must then imagine that the data are reorganized so that in every brain position there is a q-space signal sample that consists of hundreds of values and that in every brain position a Fourier transform relates the raw q-space data to the diffusion probability density function (Fig 12).

q-Space is always sampled for a specific diffusion time interval Δ, which is determined by the duration of the interval between the two gradient pulses. The diffusion time interval can be varied to enhance different properties. For example, a longer interval produces better directional resolution. Imagine diffusion within an axon: With a

very short diffusion time interval, there is a similar amount of diffusion in every direction. When the interval is longer, diffusion perpendicular to the direction of the axon stops when the molecules reach the axon wall, while diffusion along the long axis of the axon continues. Thus, a longer interval increases the distinction between the signals in different directions; however, it also leads to a lower signal-to-noise ratio.

To describe the parameters applied in sampling q-space, the term "*b* value" is often used. The *b* value is proportional to the product of the diffusion time interval and the square of the strength of the diffusion gradient. All diffusion images should be compared with a reference image that is not diffusion weighted (a standard SE image)—in other words, one for which the strength of the diffusion gradient is zero ($q = 0$ and $b = 0$).

Diffusion Spectrum Imaging

Diffusion spectrum imaging may be described as the reference standard of diffusion imaging because it is the practical implementation of the principles derived earlier and is the diffusion imaging technique that has a sound basis in physical theory (12). Suitable for in vivo application, it provides a sufficiently dense q-space signal sample from which to derive a displacement distribution with the use of the Fourier transform. The technique was first described by Wedeen et al (13).

If established practice is followed, 515 diffusion-weighted images are acquired successively, each corresponding to a different **q** vector, that are placed on a cubic lattice within a sphere with a radius of five lattice units. The lattice units correspond to different *b* (or **q**) values, from $b = 0$ (which corresponds to the centerpoint of the sphere) to, typically, $b = 12{,}000$ sec/mm^2 (which is a very high *b* value). The Fourier transform is computed over the q-space data. If the imaging matrix size is $128 \times 128 \times 30$, the same number of Fourier transform operations will be necessary as the diffusion probability density function is computed for every brain location.

Traditionally, 515 images were considered necessary to obtain data of good quality, although the acquisition of that number of images is very time consuming. With improvements in MR imaging hardware and techniques in recent years, and in view of additional very recent experience, fewer sampling points seem to be necessary; the probability density function can be reconstructed with approximately 257 or even 129 images by sampling only one hemisphere in q-space. Of course, the signal-to-noise ratio and angular resolution may change accordingly. The time for imaging of both brain hemispheres thus can be reduced from approximately 45–60 minutes to as little as 10–20 minutes, an acquisition time that makes the technique feasible in a clinical setting (14).

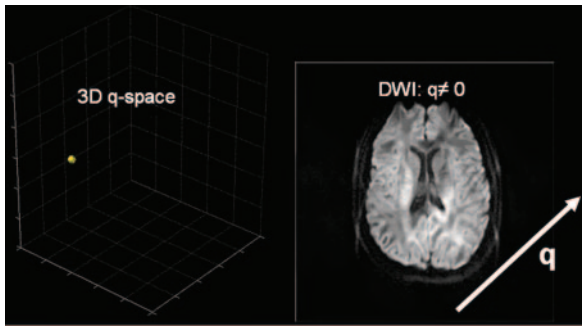

Figure 13. Diffusion-weighted image (right) from signal sampling at a single point in 3D q-space (left). Brain areas where diffusion is intense in the direction of the applied gradient ($\tilde{q}$) appear darker because of a decrease in the measured signal that results from dephasing.

With the application of the Fourier transform over q-space in every brain position, a 6D image of both position and displacement is obtained. Diffusion at each position is described by the displacement distribution or the probability density function, which provides a detailed description of diffusion and excellent resolution of the highly complex fiber organization, including fiber crossings. Since diffusion spectrum imaging is mostly used for fiber tractography, in which only directional information is needed, the probability density function is normally reduced to an orientation distribution function by summing the probabilities of diffusion in each direction (Fig 7).

From the Simplest to the Most Sophisticated Technique

Diffusion-weighted MR Imaging

Diffusion-weighted MR imaging is the simplest form of diffusion imaging. A diffusion-weighted image is one of the components needed to reconstruct the complete probability density function as in diffusion spectrum imaging. A diffusion-weighted image is the unprocessed result of the application of a single pulsed gradient SE sequence in one gradient direction, and it corresponds to one point in q-space. Even though such an image is rather simple, it does contain some information about diffusion. In Figure 13, the left splenium of the corpus callosum appears bright, whereas the right splenium appears dark. In regions such as the right splenium, where the main diffusion direction is aligned with the applied dif-

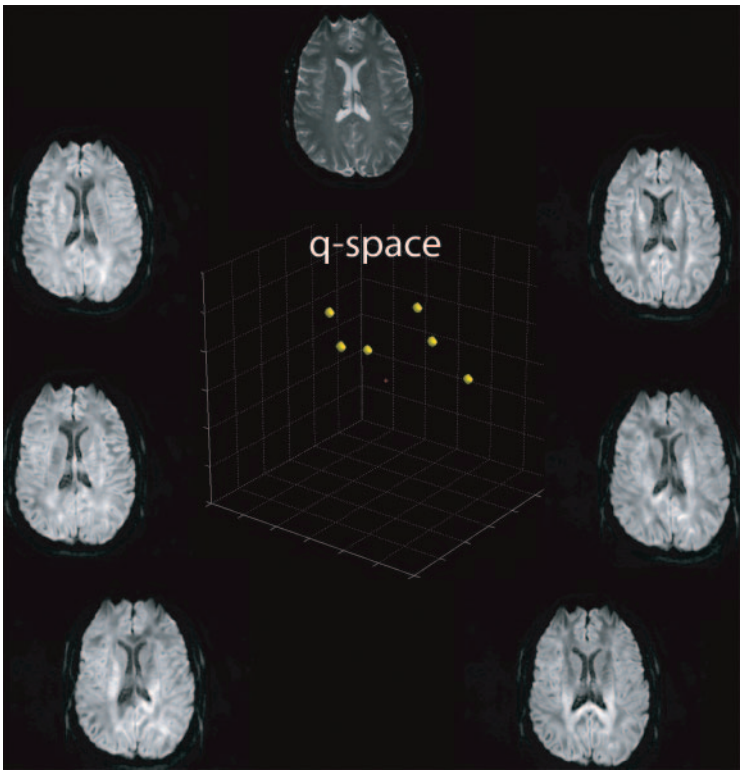

Figure 14. Series of diffusion-weighted images obtained for diffusion tensor imaging, in which q-space is sampled in at least six different directions and in which a non–diffusion-weighted reference image is obtained. The direction but not the strength of the diffusion gradient is changed for each sampling.

fusion gradient, the intensity of the signal is markedly decreased, and the region therefore appears darker on the image. In the ventricles, diffusion is free and substantial in all directions, including the applied gradient direction, and therefore the entirety of the ventricles appears dark. Despite its simplicity, diffusion-weighted imaging is routinely used in investigations of stroke (15). Indeed, in acute stroke, the local cell swelling produces increased restriction of water mobility and hence a bright imaging appearance due to high signal intensity in the area of the lesion. The benefit of diffusion-weighted imaging is that the acquisition time is short, since only one image is needed.

ADC and Trace

The problem of diffusion-weighted imaging is that the interpretation of the resultant images is not intuitive. To resolve this problem, let us assume that the diffusion has no restrictions and that its displacement distribution therefore can be described with a free-diffusion physical model, which is a 3D isotropic Gaussian distribution. In this model, the physical diffusion coefficient D is replaced by the ADC, which is derived from the equation $\text{ADC} = -b \ln(\text{DWI}/b_0)$, where DWI is the diffusion-weighted image intensity for a specific b value and diffusion gradient direction, defined as in the previous section, and b_0 is a reference image without diffusion weighting. Thus, to obtain an image of the ADC values, two acquisitions are necessary.

The ADC is very dependent on the direction of diffusion encoding. To overcome this limitation, one can perform three orthogonal measurements and average the result to obtain a better approximation of the diffusion coefficient. This method is equivalent to the derivation of the trace from the diffusion tensor, described in more detail in the next section.

Diffusion Tensor Imaging and Derived Scalars

For ADC imaging, we have assumed that diffusion follows a free-diffusion physical model and is described by an isotropic Gaussian distribution. This model often is too simplistic, especially if we are interested in the orientation of axonal bundles in which diffusion is expected to be anisotropic (ie, not the same in all directions). For purposes of discussion, then, let us assume that diffusion remains Gaussian but may be anisotropic. In other words, diffusion may be cigar or disc shaped but also may be spherical, as in isotropic diffusion. Anisotropic Gaussian distributions have six degrees of freedom instead of one. Therefore, to fit our model, we must sample at least six points in q-space with $q \neq 0$ (diffusion-weighted images) and one point with $q = 0$ (reference image) (Fig 14). In general, a b value of approximately 1000 sec/mm^2 is used. To fit the resultant data to the model, we must solve a set of

six equations like the equation given earlier. The result is a diffusion tensor (instead of a diffusion coefficient) that is proportional to the Gaussian covariance matrix (instead of the Gaussian variance) (16). This diffusion tensor is a 3 × 3 matrix that fully characterizes diffusion in 3D space, assuming that the displacement distribution is Gaussian. The diffusion tensor is usually represented by an ellipsoid or an orientation distribution function (Fig 15).

Teaching Point

The mathematical properties of the diffusion tensor make it possible to extract several useful scalar measures from diffusion tensor images. The mean diffusion, also known as the trace, is computed by averaging the diagonal elements of the matrix (16). The result is an image like that in Figure 16a and is the same as the result obtained by estimating the ADC in three orthogonal directions. The direction of the diffusion maximum is called the principal direction of diffusion and can be directly obtained by computing eigenvectors and eigenvalues of the tensor. Eigenvectors are orthogonal to one another, and, with eigenvalues, describe the properties of the tensor. Eigenvalues are ordered as $\lambda_1 \geq \lambda_2 \geq \lambda_3$, and each corresponds to one eigenvector. The eigenvector that corresponds to the largest eigenvalue (λ_1) is the principal direction of diffusion. If the eigenvalues are significantly different from each other, diffusion is said to be anisotropic (Fig 15). If λ_1 is much larger than the second eigenvalue, λ_2, the diffusion is cigar shaped (Fig 15). If λ_1 and λ_2 are similar but are much larger than λ_3, the diffusion is said to be planar or disc shaped. When all the eigenvalues are approximately equivalent, diffusion is isotropic and may be represented as a sphere (17).

The relationship between the eigenvalues reflects the characteristics of diffusion. To describe the shape of diffusion with a scalar value, fractional anisotropy is most often used (16). However, other measures, such as those described by Westin et al (17), are available. Fractional anisotropy is computed by comparing each eigenvalue with the mean of all the eigenvalues ($\langle\lambda\rangle$), as in the following equation:

$$FA = \sqrt{\frac{3}{2}}\sqrt{\frac{(\lambda_1 - \langle\lambda\rangle)^2 + (\lambda_2 - \langle\lambda\rangle)^2 + (\lambda_3 - \langle\lambda\rangle)^2}{\lambda_1^2 + \lambda_2^2 + \lambda_3^2}},$$

where FA is the fractional anisotropy. The fractional anisotropy of a section of diffusion tensors can be seen in Figure 16b.

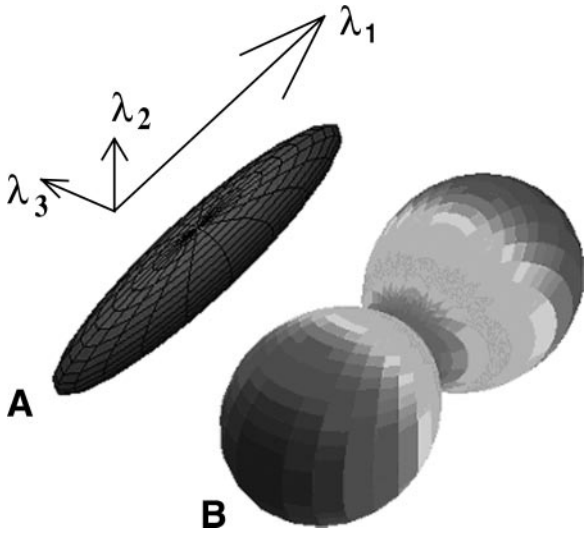

Figure 15. Diagram of diffusion tensors. In *A,* the diffusion tensor is shown as an ellipsoid (an isosurface) with its principal axes along the eigenvectors (λ_1,λ_2,λ_3). In *B,* the diffusion tensor is shown as an orientation distribution function.

The ellipsoid or the orientation distribution function is the most accurate method for visualizing the diffusion tensor data, but sometimes it is difficult to represent it over an imaging section on a display monitor (18). Color coding of the diffusion data according to the principal direction of diffusion may be a more practical way of visualizing the data (16). In the color coding system that we use, red corresponds to diffusion along the inferior-superior axis (x-axis); blue, to diffusion along the transverse axis (y-axis); and green, to diffusion along the anterior-posterior axis (z-axis). The intensity of the color is proportional to the fractional anisotropy. An example of this color coding scheme is shown in Figure 16c.

The diffusion tensor model performs well in regions where there is only one fiber population (ie, fibers are aligned along a single axis), where it gives a good depiction of the fiber orientation. However, it fails in regions with several fiber populations aligned along intersecting axes because it cannot be used to map several diffusion maxima at the same time. In such areas, imaging techniques that provide higher angular resolution are needed.

Teaching Point

Diffusion Tensor Imaging and Diffusion Spectrum Imaging

Because of the limited number of applied diffusion gradients and degrees of freedom, the diffusion tensor model is incapable of resolving fiber crossings. In contrast, diffusion spectrum imaging

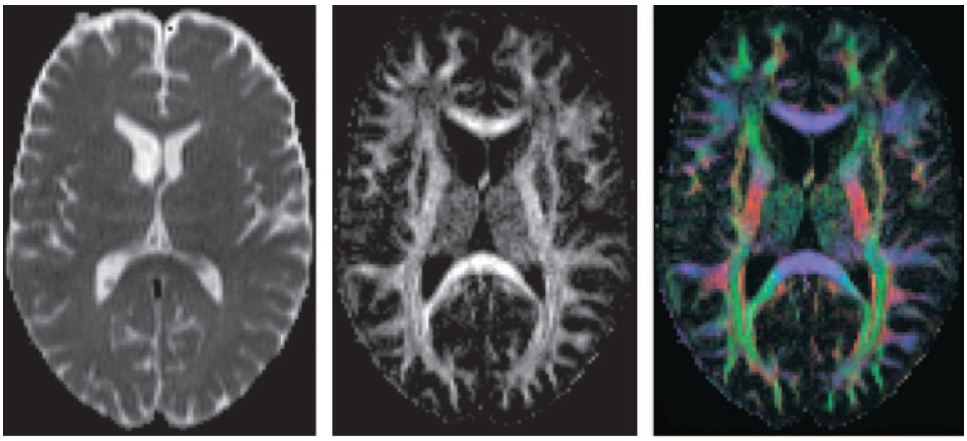

a. b. c.

Figure 16. Extraction of scalar values from diffusion tensor imaging. **(a)** Image shows mean diffusion, which is the trace of the diffusion tensor. An image of ADC averaged over three orthogonal directions would have a similar appearance. **(b)** Image shows the fractional anisotropy, which is computed from the eigenvalues of the diffusion tensor. **(c)** Color-coded image shows the orientation of the principal direction of diffusion, with red, blue, and green representing diffusion along x-, y-, and z-axes, respectively. The color intensity is proportional to the fractional anisotropy.

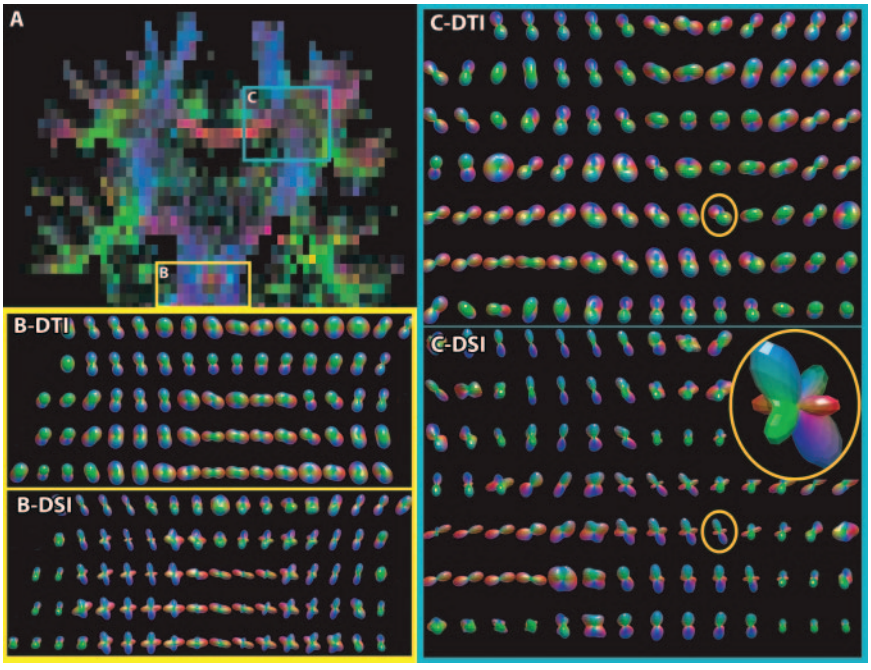

Figure 17. Comparison between diffusion tensor and diffusion spectrum imaging in regions that contain fiber crossings. In *A*, a color-coded coronal diffusion image shows the pons *(B)* and the centrum semiovale *(C)*, in which diffusion is depicted by both diffusion tensor images *(B-DTI, C-DTI)* and diffusion spectrum images *(B-DSI, C-DSI)*. In the pons, the middle cerebellar peduncle crosses the corticospinal tract. In the centrum semiovale, the corticospinal tract crosses the corpus callosum and the arcuate fasciculus. In the circled sections *(C-DTI, C-DSI)*, it can be seen that diffusion tensor imaging is not capable of resolving fiber crossings, whereas diffusion spectrum imaging is.

is not predicated on any particular hypothesis concerning diffusion. Accordingly, its capability to resolve the diffusion probability density function depends only on the resolution in q-space, and its capability to resolve fiber crossings depends only on the related angular resolution. In Figure 17, images obtained with the two methods are juxtaposed. The regions in which the most striking difference can be seen are the pons, where the corticospinal tract and middle cerebellar peduncle cross, and the centrum semiovale,

where the corticospinal tract crosses the corpus callosum and the arcuate fasciculus.

With regard to acquisition times, diffusion tensor imaging has a clear advantage over diffusion spectrum imaging in that it requires a minimum of only seven images, whereas diffusion spectrum imaging requires several hundred images. Diffusion spectrum imaging previously involved long acquisition times, but with constant improvements the acquisition time is decreasing (14).

Increased Angular Resolution with q-Ball Imaging

We have seen, on one hand, that diffusion tensor imaging is insufficient in many brain areas for accurately mapping the orientation of major tracts. On the other hand, we would like to have available a faster technique than diffusion spectrum imaging, which is time consuming for routine clinical applications, although improvements in this regard are currently being evaluated. q-Ball imaging is an attempt to combine the best attributes of these two techniques (19). Although we decided for illustrative purposes to discuss q-ball imaging only, there are many other heuristic methods, such as those based on persistent angular structure (20) and spherical deconvolution (21). All these techniques are based on an identical or nearly identical scheme that consists of rather dense sampling of the signal within a sphere with a constant high *b* value in q-space. The orientation distribution function is estimated from the resultant data by using various algorithms.

Like diffusion tensor imaging, q-ball imaging is based on a hypothesis about the shape of the diffusion probability density function. This hypothesis is complex and demands a more in-depth consideration of the spatial frequency content of the signal in q-space than can be provided in the present article. Here, we consider only a specific type of diffusion probability density function for which q-ball imaging provides an adequate basis. We assume that the compartments inside a voxel consist of a set of straight and very thin pipes with impermeable walls. Water molecules inside the pipes are assumed to diffuse uniformly along the length of the pipes but to have no transverse motion. The diffusion probability density function in this case would look like a pincushion. With this model, diffusion can be reconstructed by sampling points in q-space on a sphere with a constant radius, at a high *b* value (typically, >4000 sec/mm^2). The data are reconstructed by using the Funk-Radon transform, an algorithm that can be described as follows: Suppose that we want to know the diffusion intensity (ie, the value of the orientation distribution function) in a direction that corresponds to the North Pole and that the MR signal has been sampled over the globe. If we add together the values of the signal intensity measured along the equator, the sum will be proportional to the diffusion intensity at the North Pole. If we redefine the location of the North Pole as, for example, Lausanne and redefine the equator accordingly, the value of the orientation distribution function at Lausanne can be computed in a similar fashion. The same can be done to reconstruct the orientation distribution function for any point (eg, Boston, Stockholm, Brussels) on the globe (Fig 18).

Unlike diffusion tensor imaging, q-ball imaging can account for multiple crossing fibers within a single voxel and therefore can provide realistic depiction of areas of complex fiber architecture, such as the centrum semiovale and the pons. With q-ball imaging, the images obtained resemble those acquired with diffusion spectrum imaging. However, further validation studies must be performed to determine whether q-ball imaging provides high-quality depiction of all regions of the brain and whether the reconstructed images are accurate.

Diffusion MR Tractography

Brain fiber tractography is a rendering method for improving the depiction of data from diffusion imaging of the brain. Although a detailed discussion of tractography is beyond the scope of this article, a short introduction is necessary because tractography is one of the most powerful tools developed to aid image interpretation. The primary purpose of tractography is to clarify the orientational architecture of tissues by integrating pathways of maximum diffusion coherence. Fibers are grown across the brain by following from

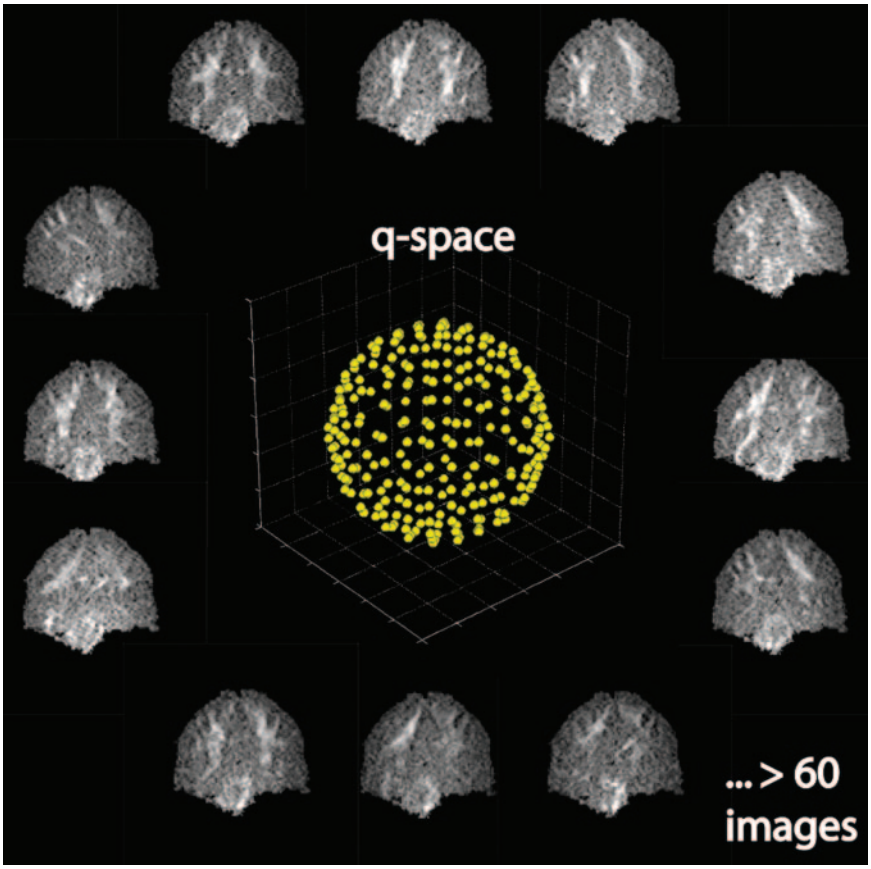

Figure 18. Diagram shows that in q-ball imaging, points on a shell with a constant *b* value are acquired in q-space. At least 60 images are necessary to reconstruct an orientation distribution function that is realistic.

voxel to voxel the direction of the diffusion maximum. The fibers depicted with tractography are often considered to represent individual axons or nerve fibers, but they are more correctly viewed in physical terms as lines of fast diffusion that follow the local diffusion maxima and that only generally reflect the axonal architecture. This distinction is useful because, for a given imaging resolution and signal-to-noise ratio, lines of maximum diffusion coherence (ie, the computer-generated fibers) may differ from the axonal architecture in some brains. Tractography adds information and interest to the MR imaging depiction of the human neuronal anatomy.

The connectivity maps obtained with tractography vary according to the diffusion imaging modality used to obtain the diffusion data. For example, diffusion tensor imaging provides a Gaussian approximation of the actual displacement distribution, and since the representation of that distribution is restricted to variations of an ellipsoid, this method creates various biases in the tractography result. In contrast, diffusion spectrum imaging with tractography overcomes many of those biases and allows more realistic mapping of connectivity. The tractography result also depends on the tracking algorithm used. Deterministic fiber tracking from diffusion tensor imaging uses the principal direction of diffusion to integrate trajectories over the image (22) but ignores the fact that fiber orientation is often undetermined in the diffusion tensor imaging data. To overcome this limitation of the data, Hagmann and colleagues, as well as other investigators, investigated statistical fiber tracking methods based on consideration of the tensor as a probability distribution of fiber orientation (23–25).

The application of fiber tractography to data such as those obtained with diffusion spectrum imaging or q-ball imaging results in the depiction of a large set of fiber tracts with a more complex

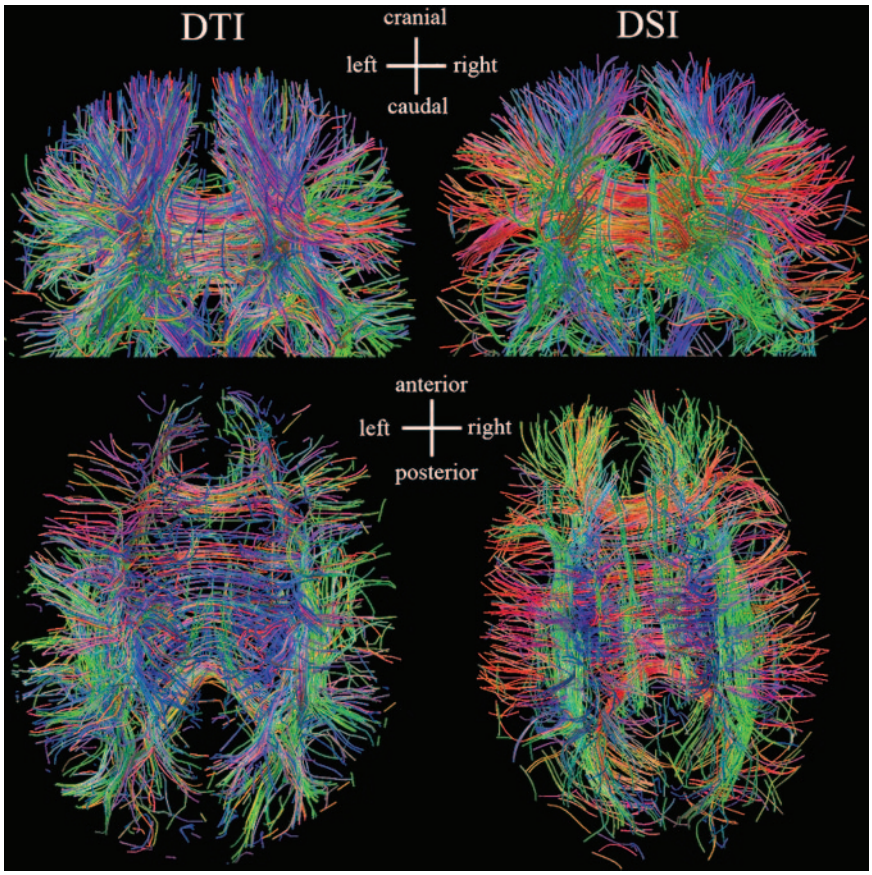

Figure 19. Comparison of fiber tractography based on diffusion tensor imaging *(DTI)* versus fiber tractography based on diffusion spectrum imaging *(DSI)* in two healthy volunteers. The diffusion spectrum imaging data were obtained with a 3.0-T imager and a twice-refocused SE pulse (repetition time msec/echo time msec = 3000/154; b_{max} = 17,000 sec/mm^2; voxel size of 3 × 3 × 3 mm); tractography was performed according to the method described in reference 26. The diffusion tensor imaging data were obtained with a 1.5-T imager and a single-shot echo-planar sequence (1000/89; b = 1000 sec/mm^2; voxel size of 1.64 × 1.64 × 3 mm); tractography was performed as described in reference 23. Because diffusion spectrum imaging provides higher angular resolution, fiber crossings are better resolved and fibers from different tracts are more clearly separated. The most visible differences between the two axial views (bottom row) are the greater predominance of red, which represents decussating callosal fibers that connect both the parietal and the temporal lobes, and the more uniform distribution of callosal fibers that project into the frontal lobe, on the diffusion spectrum image. These differences reflect typical errors of diffusion tensor imaging tractography in areas where fibers cross.

geometry (26). The greater complexity obtained with this method, compared with that from tractography with diffusion tensor MR imaging data, is due to the consideration of numerous intersections between fibers that can be resolved or differentiated. The difference between tractography performed with diffusion tensor imaging data and tractography performed with diffusion spectrum imaging data can be seen in Figure 19.

Conclusions

Water diffusion is produced by the random motion of water molecules because of thermal energy. The molecular displacement depicted at diffusion MR imaging is best described at the level of a selected molecular population—typically, the water molecules contained in a voxel—by calculating the probability density function or displacement distribution. The 3D diffusion probability density function is shaped by local tissue structure, which hinders molecular displacement. Because biological tissue is heterogeneous, with a different tissue architecture in

Table 1
Technical Requirements of Diffusion MR Imaging Techniques

Technique and Reference	3.0 T and High Gradient Strength Capabilities	No. of Gradient Directions	Maximal Gradient Strength (sec/mm^2)	Acquisition Time (min)*	Postprocessing	Display
Diffusion-weighted imaging (15)	Optional	1	≤1000	1–3	None	Gray-scale sections
Trace and ADC imaging (16)	Optional	≥3	≤1000	2–4	Simple summation, usually performed automatically by the imaging system	Gray-scale sections
Diffusion tensor imaging (16)	Optional	≥6	≤1000	3–6	Simple matrix operation, usually performed automatically by the imaging system	Gray-scale sections for derived scalars (eg, trace, fractional anisotropy), color-coded sections for diffusion direction, ellipsoid reconstruction of orientation distribution function, tractography
q-Ball imaging (19)	Desirable	≥60	>4000	10–20	Complex filtered back-projection with many parameters	Trace, general fractional anisotropy, orientation distribution function, tractography
Diffusion spectrum imaging (12)	Very desirable	≥200	>8000	15–60	Complex (filtered Fourier transform and radial projection with multiple parameters)	Trace, general fractional anisotropy, probability density function, orientation distribution function, tractography

*It is assumed that 30 axial sections are acquired, each with a thickness of 3 mm.

different anatomic positions, a 3D displacement distribution must be calculated for every 3D voxel, to produce a 6D image that depicts both position and displacement. This 6D image is best obtained with diffusion spectrum imaging, the reference standard. Diffusion spectrum imaging is a rather complex and demanding technique (Table 1), with stringent hardware requirements. Many simpler diffusion imaging techniques also exist that can provide important information about diffusion and tissue structure; however, the information they provide is partial and often hypothesis based, and those who use such techniques must be aware of their limitations. Imaging of the ADC and trace are extremely simple methods and provide only basic information, namely an estimate of the variance of the diffusion function. Diffusion tensor imaging and q-ball imaging are hypothesis-based simplifications that are used to shorten image acquisition time and reduce hardware requirements. Like diffusion spectrum imaging, they can be used to obtain maps of the orientation distribution functions. Care must be taken when interpreting diffusion

Table 2
Advantages and Drawbacks of Diffusion MR Imaging Techniques

Technique	Information Obtained	Advantages	Drawbacks
Diffusion-weighted imaging	Diffusion measurement in one direction	Short acquisition time, no postprocessing, images easy to interpret. Examination well tolerated by patients. Adequate hardware capabilities readily available.	Provides unidirectional diffusion measurement only, limited information. Voxel intensity is not a natural physical unit but a measure of restriction.
Trace and ADC imaging	Estimated diffusion coefficient	Short acquisition time, nearly no (or automated) postprocessing, images easy to interpret. Voxel intensity has physical meaning. Examination well tolerated by patients. Adequate hardware capabilities readily available.	Hypothesis based (hypothesis not always true). Limited information (no measurement of orientation or anisotropy).
Diffusion tensor imaging	Estimated diffusion tensor	Short acquisition time, some postprocessing required (automated on recent imaging systems). Provides information about diffusion orientation and anisotropy. Examination well tolerated by patients. Adequate hardware capabilities readily available.	Hypothesis based (hypothesis not always true). Does not provide accurate map of complex fiber architecture. Tractography results are vulnerable to severe artifacts.
q-Ball imaging	Estimated map of orientation distribution function values	Feasible with reasonable acquisition time. Provides information about diffusion orientation and anisotropy, accurate depiction of fiber crossings. Examination tolerated by most patients.	Hypothesis based. Although results seem correct in important brain areas, accuracy is not guaranteed in all brain regions. Further validation is required. Hardware requirements are high.
Diffusion spectrum imaging	Full 3D diffusion probability density function map, true 6D images	Principle based, hypothesis free, has already received theoretical and practical validation. Provides accurate depiction of fiber crossings with a specific angular resolution. Maps the entire field of diffusion, providing 6D data and increasing the possibility of quantitation. Provides diffusion tensor information.	Hardware requirements are high, and acquisition time is comparatively long. Whole-brain studies were not tolerable for patients. Recent improvements in hardware and imaging techniques have made shorter acquisition times possible, allowing future patient studies.

tensor imaging data and q-ball imaging data, as there may be brain areas in which the underlying hypotheses are not applicable, whereas diffusion spectrum imaging is limited only by factors such as k- and q-space resolution and signal-to-noise ratio. Tractography is a visualization technique that can be used to extract lines of maximum diffusion coherence from any orientation distribution function map. These lines reflect the anat-

omy of the axonal trajectories. Many uses are foreseen for fiber tractography, from single-tract analysis to whole-brain connectivity analysis (27,28). The technical requirements and the results that can be achieved with each diffusion MR imaging method are described in Table 1. The radiologist should weigh the pros and cons (Table 2) of each technique and, depending on the question addressed and the equipment available, choose the most adequate. It is our hope that the information in this article will be helpful in making that decision.

References

1. Einstein A. Investigations on the theory of the brownian movement. New York, NY: Dover, 1956.
2. Le Bihan D. Looking into the functional architecture of the brain with diffusion MRI. Nat Rev Neurosci 2003;4:469–480.
3. Lin CP, Wedeen VJ, Chen JH, Yao C, Tseng WY. Validation of diffusion spectrum magnetic resonance imaging with manganese-enhanced rat optic tracts and ex vivo phantoms. Neuroimage 2003; 19:482–495.
4. Beaulieu C. The basis of anisotropic water diffusion in the nervous system: a technical review. NMR Biomed 2002;15:435–455.
5. Hahn E. Spin echoes. Phys Rev 1950;80:580–594.
6. Torrey H. Bloch equations with diffusion terms. Phys Rev 1956;104:563–565.
7. Stejskal E, Tanner J. Spin diffusion measurements: spin echoes in presence of a time-dependent field gradient. J Chem Phys 1965;42:288.
8. Pooley RA. AAPM/RSNA physics tutorial for residents: fundamental physics of MR imaging. RadioGraphics 2005;25:1087–1099.
9. Poustchi-Amin M, Mirowitz SA, Brown JJ, McKinstry RC, Li T. Principles and applications of echo-planar imaging: a review for the general radiologist. RadioGraphics 2001;21:767–779.
10. Glockner JF, Hu HH, Stanley DW, Angelos L, King K. Parallel MR imaging: a user's guide. RadioGraphics 2005;25:1279–1297.
11. Callaghan PT. Principles of nuclear magnetic resonance microscopy. Oxford, England: Clarendon, 1991.
12. Wedeen VJ, Hagmann P, Tseng WY, Reese TG, Weisskoff RM. Mapping complex tissue architecture with diffusion spectrum magnetic resonance imaging. Magn Reson Med 2005;54:1377–1386.
13. Wedeen V, Reese T, Tuch D, et al. Mapping fiber orientation spectra in cerebral white matter with Fourier-transform diffusion MR [abstract]. In: Proceedings of the Eighth Meeting of the International Society for Magnetic Resonance in Medicine. Berkeley, Calif: International Society for Magnetic Resonance in Medicine, 2000; 82.
14. Reese TG, Benner T, Wang R, Feinberg DA, Wedeen VJ. Halving imaging time of whole brain diffusion spectrum imaging (DSI) by using simultaneous echo refocusing (SER) EPI [abstract]. In: Proceedings of the Fourteenth Meeting of the International Society for Magnetic Resonance in Medicine. Berkeley, Calif: International Society for Magnetic Resonance in Medicine, 2006; 1044.
15. Roberts TP, Rowley HA. Diffusion weighted magnetic resonance imaging in stroke. Eur J Radiol 2003;45:185–194.
16. Le Bihan D, Mangin JF, Poupon C, et al. Diffusion tensor imaging: concepts and applications. J Magn Reson Imaging 2001;13:534–546.
17. Westin CF, Maier SE, Mamata H, Nabavi A, Jolesz FA, Kikinis R. Processing and visualization for diffusion tensor MRI. Med Image Anal 2002; 6:93–108.
18. Basser PJ, Mattiello J, LeBihan D. MR diffusion tensor spectroscopy and imaging. Biophys J 1994; 66:259–267.
19. Tuch DS, Reese TG, Wiegell MR, Wedeen VJ. Diffusion MRI of complex neural architecture. Neuron 2003;40:885–895.
20. Jansons KM, Alexander DC. Persistent angular structure: new insights from diffusion MRI data. Dummy version. Inf Process Med Imaging 2003; 18:672–683.
21. Tournier JD, Calamante F, Gadian DG, Connelly A. Direct estimation of the fiber orientation density function from diffusion-weighted MRI data using spherical deconvolution. Neuroimage 2004; 23:1176–1185.
22. Mori S, van Zijl PC. Fiber tracking: principles and strategies—a technical review. NMR Biomed 2002;15:468–480.
23. Hagmann P, Thiran JP, Jonasson L, et al. DTI mapping of human brain connectivity: statistical fibre tracking and virtual dissection. Neuroimage 2003;19:545–554.
24. Parker GJ, Haroon HA, Wheeler-Kingshott CA. A framework for a streamline-based probabilistic index of connectivity (PICo) using a structural interpretation of MRI diffusion measurements. J Magn Reson Imaging 2003;18:242–254.
25. Behrens TE, Woolrich MW, Jenkinson M, et al. Characterization and propagation of uncertainty in diffusion-weighted MR imaging. Magn Reson Med 2003;50:1077–1088.
26. Hagmann P, Reese T, Tseng W, Meuli R, Thiran J, Wedeen V. Diffusion spectrum imaging tractography in complex cerebral white matter: an investigation of the centrum semiovale [abstract]. In: Proceedings of the Twelfth Meeting of the International Society for Magnetic Resonance in Medicine. Berkeley, Calif: International Society for Magnetic Resonance in Medicine, 2004; 623.
27. Hagmann P. From diffusion MRI to brain connectomics [PhD dissertation]. Lausanne, Switzerland: Signal Processing Institute, École Polytechnique Fédérale de Lausanne (EPFL), 2005.
28. Hagmann P, Kurant M, Gigandet X, et al. Imaging the brain neuronal network with diffusion MRI: a way to understand its global architecture [abstract]. In: Proceedings of the Fourteenth Meeting of the International Society for Magnetic Resonance in Medicine. Berkeley, Calif: International Society for Magnetic Resonance in Medicine, 2006; 436.

Understanding Diffusion MR Imaging Techniques: From Scalar Diffusion-weighted Imaging to Diffusion Tensor Imaging and Beyond

Patric Hagmann, MD, PhD et al

RadioGraphics 2006; 26:S205–S223 • **Published online** 10.1148/rg.26si065510 • **Content Codes:** MR NR PH

Page S206
In a glass of water, the motion of the water molecules is completely random and is limited only by the boundaries of the container. This erratic motion is best described in statistical terms by a displacement distribution. The displacement distribution describes the proportion of molecules that undergo displacement in a specific direction and to a specific distance.

Page S209
A defining characteristic of neuronal tissue is its fibrillar structure. Neuronal tissue consists of tightly packed and coherently aligned axons that are surrounded by glial cells and that often are organized in bundles. As a result, the micrometric movements of water molecules are hindered to a greater extent in a direction perpendicular to the axonal orientation than parallel to it.

Page S210
An orientation distribution function may be considered a deformed sphere whose radius in a given direction is proportional to the sum of values of the diffusion probability density function in that direction.

Page S216

This diffusion tensor is a 3×3 matrix that fully characterizes diffusion in 3D space, assuming that the displacement distribution is Gaussian. The diffusion tensor is usually represented by an ellipsoid or an orientation distribution function.

Pages S216
The diffusion tensor model performs well in regions where there is only one fiber population (ie, fibers are aligned along a single axis), where it gives a good depiction of the fiber orientation. However, it fails in regions with several fiber populations aligned along intersecting axes because it cannot be used to map several diffusion maxima at the same time. In such areas, imaging techniques that provide higher angular resolution are needed.